CT1000S AC/DC Split Core Current Sensor

Hiroyuki Ishida [*1] *Hiroyuki Degawa* [*2] *Hiroki Minami* [*1]

The CT1000S AC/DC split-core current sensor with a split sensor part has been developed. It has a rated current of 1000 A, an operating temperature range of −40 to 85°C, an amplitude accuracy (0.1 Hz to 100 Hz) of ±0.2% of reading and ±0.01% of full scale, and a frequency bandwidth of DC to 300 kHz (−3 dB). Despite having a divisible structure, it is a high-accuracy, high-bandwidth voltage output current sensor for split-core type current sensors.

The divisible structure of the sensor part allows a cable to be easily threaded through its measurement through-hole, making it possible to measure currents in applications where the cable cannot be disconnected. To improve measurement reproducibility, the sensor is designed to be placed stably on the floor, screw holes are provided to fix the current sensor body, and a conductor position adjuster can limit the cable position.

This paper introduces the features of the CT1000S AC/DC split-core current sensor and the technologies realized in its development.

INTRODUCTION

The industrial sector has long been working to improve the energy efficiency of equipment in order to realize a decarbonized society[(1)]. Enhancing the energy efficiency of power converters and battery management systems is an effective way to utilize electric power more efficiently. However, highly accurate power measurement is required to achieve this[(2)(3)].

When measuring current in finished products or equipment, it is often difficult to disconnect or cut the cables, so a split-core current sensor is used. The CT1000S AC/DC split-core current sensor (hereinafter, "CT1000S") is a split-core sensor that allows for easy attachment and detachment to the measurement cable. Although the measurement accuracy of typical split-core current sensors is generally low, the CT1000S can measure current with high accuracy. Furthermore, with a small phase error of ±0.1°, it can be used as a current sensor for power measurement, and it is also suitable for waveform measurement due to its low output noise.

Figure 1 shows the appearance of the CT1000S. By incorporating mechanisms that enhance measurement reproducibility, the CT1000S combines the convenience of a split-core structure with high measurement reproducibility. This paper introduces the features of the CT1000S, and the technologies developed in its design.

*1 Decarbonization Business Division, Yokogawa Test & Measurement Corporation
*2 Common Technology & QA Division, Yokogawa Test & Measurement Corporation

Figure 1 Appearance of the CT1000S

FEATURES OF THE CT1000S

Concept

High-accuracy non-contact current sensors are generally classified into clamp-type and through-type sensors. Clamp-type sensors have an open-close mechanism in the sensor unit to facilitate attachment to cables. This mechanism inevitably decreases the reproducibility of the sensor position before and after opening, but this results in lower measurement accuracy and reproducibility in comparison with through-type sensors.

Despite being a clamp-type sensor, the CT1000S was developed with the goal of achieving measurement accuracy and reproducibility comparable to those of through-type sensors by incorporating design features that enhance the reproducibility of the sensor position. The specific design features are as follows.

- A floor-mounted stable structure with a flat section
- Mounting screw holes (×6)
- Conductor position limit adjuster
- Split-section interlocking structure

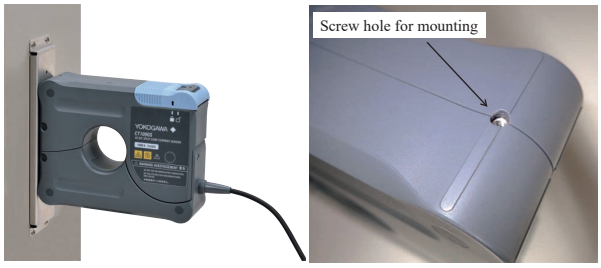

Figure 2 Usage example of screw holes for mounting

Figure 3 Split-section interlocking structure

The measurement values of non-contact current sensors are affected by the position of the measurement conductor, such as the cable, and by external magnetic fields. Therefore, fixing the positional relationship between the current sensor and the measurement conductor can improve reproducibility.

Figure 2 shows an example of the CT1000S installed using its mounting screw holes. Fixing the CT1000S in place with screws enhances measurement reproducibility.

Figure 3 shows the interlocking structure of the CT1000S split section. By adopting a floating structure with cushioning material, changes in the interlocking alignment before and after opening are prevented, thereby improving measurement reproducibility.

The CT1000S was developed with the concept of enabling users to measure current more easily and with higher accuracy. It can be applied not only to finished products and equipment, but also to applications that conventionally use through-type sensors.

Performance: Temperature Characteristics

The CT1000S consists of a main unit, subunit, and IV unit. The operating temperature range for the subunit and IV unit is 5°C to 40°C, while the main unit, which contains the sensor section, operates over a temperature range of −40°C to 85°C, allowing current to be measured under a wide range of temperature conditions.

Figure 4 shows the temperature characteristics of the CT1000S. When the ambient temperature of the main unit is between 0°C and 40°C, the specification for the primary current equivalent offset under no input is within ±0.2 A, and the worst-case measured value at 0°C was 0.02 A (Figure 4, top). When the input current is 1000 A at 50 Hz, the specification for output error is within ±0.21% of reading, and the worst-case measured value at 0°C was 0.0043% of reading (Figure 4, bottom). Since a fluxgate (FG) sensor is used to detect current from direct current (DC) to the low-frequency range, the CT1000S demonstrates stable performance against changes in ambient temperature.

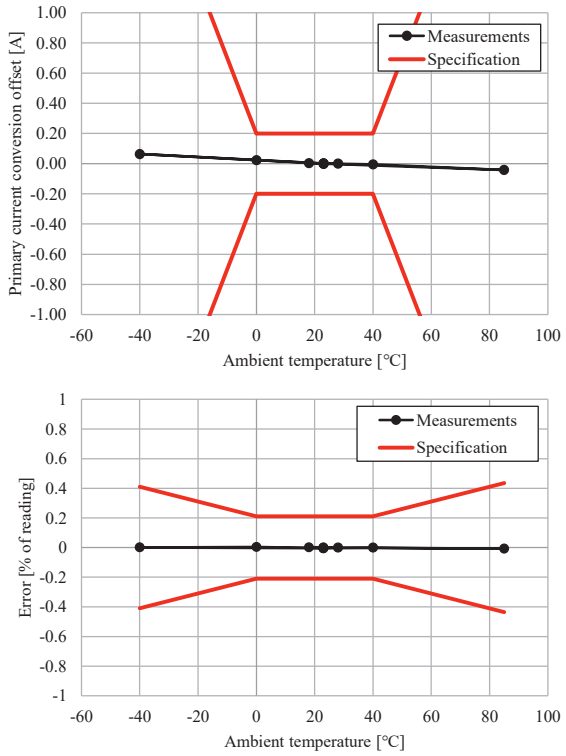

Figure 4 Output offset current with no input (top), temperature characteristics of output error with input current of 1000 A/50 Hz (bottom)

Performance: Frequency Characteristics

Figure 5 shows the amplitude frequency characteristics of the CT1000S. The sensor has an amplitude specification of within ±5.0% of reading, while the actual measurement was 0.63%, demonstrating favorable characteristics even at high frequencies. Since flatness is excellent across a wide frequency range, the sensor can be used not only for DC but also for analyzing inverter carrier frequencies and high-frequency components.

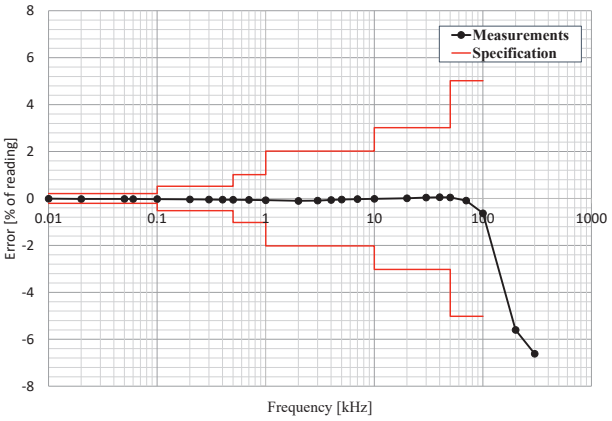

Figure 5 Amplitude frequency characteristics

Performance: Phase Characteristics

Figure 6 shows the phase frequency characteristics of the CT1000S. In the frequency range up to 0.1 kHz, the phase error specification is within ±0.1°, while the actual measurement was −0.03°.

Since the phase error is small, the CT1000S can be used in combination with a power meter to measure power with high accuracy. Some power meters are equipped with a phase correction function that compensates for the delay between the voltage input and the current input. The actual measurement in Figure 6 (after correction) represents the phase error when this function is used. Compared with the uncorrected case, the phase error is significantly reduced even in the high-frequency range. In other words, power can be measured with higher accuracy by using the phase correction function.

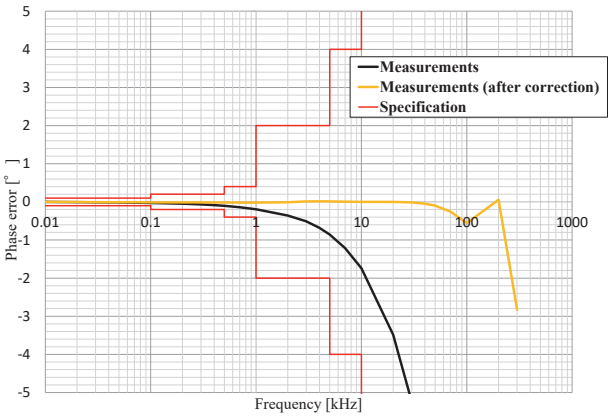

Figure 6 Amplitude frequency characteristics

Performance: DC Characteristics

Figure 7 shows the DC characteristics of the CT1000S. At the rated current of 1000 A, the DC characteristic specification is within ±0.21%, while the actual measurement was 0.021%. Due to its excellent linearity, the CT1000S can measure currents from low to high amplitude with high accuracy.

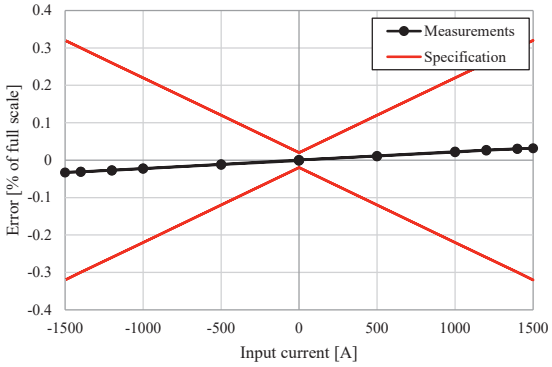

Figure 7 DC characteristics

Combination with Measuring Instruments

When used in combination with a power meter, the CT1000S can achieve high-accuracy measurement even for low-amplitude currents by utilizing the null function, which cancels the offset of the current sensor.

When used with waveform measurement instruments such as oscilloscopes, the CT1000S offers a higher signal-to-noise ratio compared to typical current sensors that use FG sensors, due to its low output noise, allowing measurement of low-amplitude waveforms.

Performance: Noise Tolerance

Figure 8 shows the common mode rejection ratio (CMRR) characteristics, which are an indicator of the noise tolerance of the CT1000S. In this paper, CMRR refers to the ratio of the primary conductor voltage to the sensor output voltage. The CMRR specification is below −100 dB at 50 kHz, while the actual measurement was −133 dB. The CMRR characteristics are good across both low and high-frequency ranges, due to the effect of the electrostatic shield shown in Figure 9.

In recent years, the increasing speed of switching devices has led to higher inverter switching speeds[2]. In inverter phase current measurements, the voltage of the conductor carrying the measured current also changes rapidly, so a high CMRR is required for current sensors. The CMRR characteristics of the CT1000S demonstrate that it can achieve high waveform repeatability in inverter measurements where the signal contains such high-frequency components.

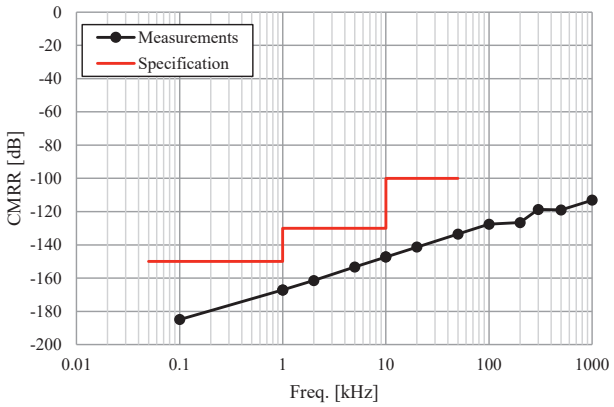

Figure 8 CMRR characteristics

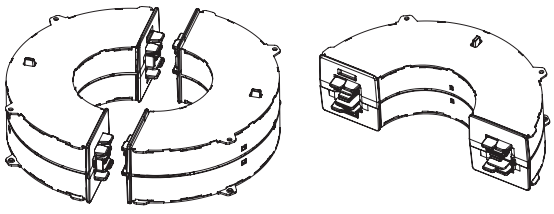

Figure 9 Electrostatic shield structure

CT1000S TECHNICAL OVERVIEW

Current Detection Method

Figure 10 shows the relationship between the frequency range of currents detected by the CT1000S and the respective current detection methods. In the alternating current (AC) region, current is detected based on the principle of a current transformer, which converts the primary current into a secondary current according to the winding ratio. For DC to low-frequency currents that cannot be detected by this method, the FG method is used. Unlike the Hall element method, the FG method does not use semiconductors in the sensor section, making it stable against temperature changes and providing excellent long-term stability. The CT1000S adopts a zero-flux method, in which no magnetic flux remains inside the magnetic core. As shown in the block diagram in Figure 11, the zero-flux method is a negative feedback system configured so that the magnetic flux in the core becomes zero. Specifically, the operation proceeds as follows:

- The primary current I_1 generates magnetic flux Φ_{I1} within the magnetic core.
- When the flux Φ_{I1} in the core is detected by the FG sensor, a current is applied to the secondary winding to generate flux Φ_{I2} that cancels the core flux. Due to the high gain of the FG sensor output at this time, $\Phi_{I1} = \Phi_{I2}$ in effect, resulting in complete cancellation of the magnetic flux in the core.
- By using the result of the IV conversion of current I_2 flowing through the secondary winding as the sensor output, a sensor output proportional to the primary current I_1 is obtained.

Through this operation, the magnetic flux in the core is minimized, which suppresses the effects of magnetic material nonlinearity and enables highly accurate current measurement.

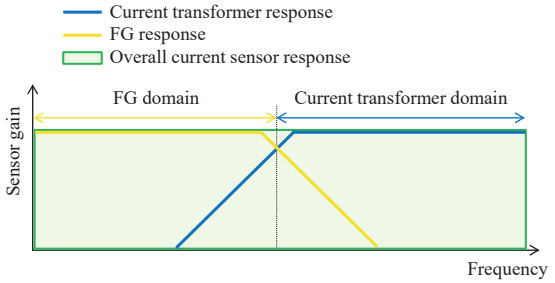

Figure 10 Relationship between frequency of current detected and current detection method

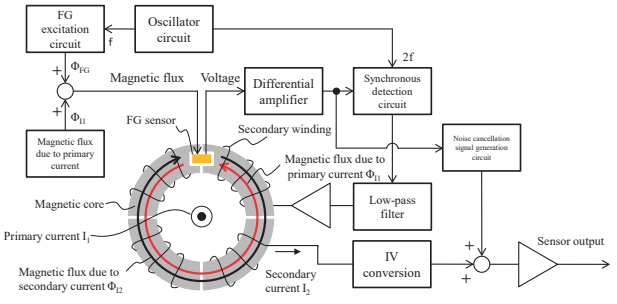

Figure 11 Block diagram

FG Sensor Using a Flexible Printed Circuit

In developing the CT1000S, an FG sensor composed of a flexible printed circuit (FPC) was created. Figure 12 shows a schematic diagram of the sensor. The features of this FG sensor are as follows:

- Protected magnetic material for easy manual handling
- Small variation in characteristics during mass production
- Simple sensor assembly by connection of connectors
- Flexible shape and easy to increase sensitivity of magnetic flux detection
- A thin profile that enables high design freedom for pairing with magnetic materials
- High durability against bending, with strong resistance to bending stress during sensor opening and closing

In structures where magnetic material is embedded in a standard FPC, poor temperature characteristics have been an issue. Therefore, in the CT1000S, the FPC structure was devised to achieve favorable temperature characteristics. The next section explains the operating principle of the FG sensor and then introduces design improvements.

Figure 12 Schematic diagram of FG sensor made from FPC

Operating Principle of the FG Sensor

Figure 13 shows a schematic diagram of the FG sensor, which consists of a thin-strip magnetic material wound with coils. It is positioned so that the magnetic flux generated by the primary current passes through the interior of the magnetic material. The FG winding is connected to and driven by an AC signal source that is controlled to maintain a constant current. Since the magnetic material is thin, it is prone to magnetic saturation, and the waveform of the excitation voltage generated in the FG winding becomes distorted. Figures 14 and 15 show examples of driving the FG winding with a triangular AC current. In these examples, magnetic saturation occurs at the peak of the excitation voltage. Figure 14 shows the excitation voltage waveform when no DC magnetic flux is applied by the primary current. The excitation voltage waveform is symmetrical in the positive and negative directions and contains only the fundamental wave and its odd-order harmonics. A synchronous detection circuit multiplies the excitation voltage waveform by a detection signal with a frequency twice the excitation frequency, but since the frequencies differ, the average value of the resulting post-detection waveform is zero.

Figure 15 shows the excitation voltage waveform when a DC magnetic flux is applied by the primary current. Focusing on the time between the current zero-crossing and the voltage peak, it is found that the timing at which the magnetic material begins to saturate differs from that in Figure 14, where no DC flux is applied. This is due to the DC magnetic flux from the primary current being superimposed on the excitation magnetic flux. The waveform also lacks positive–negative symmetry and contains a second-order harmonic, which is an even-order component. When this second harmonic is multiplied by a detection signal with twice the excitation frequency, the resulting post-detection waveform includes both a DC component and a fourth harmonic of the excitation frequency. This can be verified using the trigonometric identity $\sin(2\omega t)\cdot\sin(2\omega t) = \{\cos(0) - \cos(4\omega t)\}/2$. By passing this waveform through a low-pass filter to remove the fourth harmonic, a voltage proportional to only the DC flux component generated by the primary current is obtained. The FG sensor modulates the DC magnetic flux at twice the excitation frequency, thereby eliminating the effects of the magnetic material's temperature characteristics and circuit DC drift and enabling excellent DC performance.

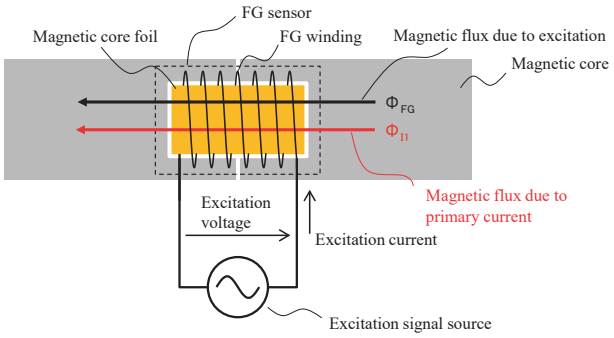

Figure 13 Schematic diagram of FG sensor

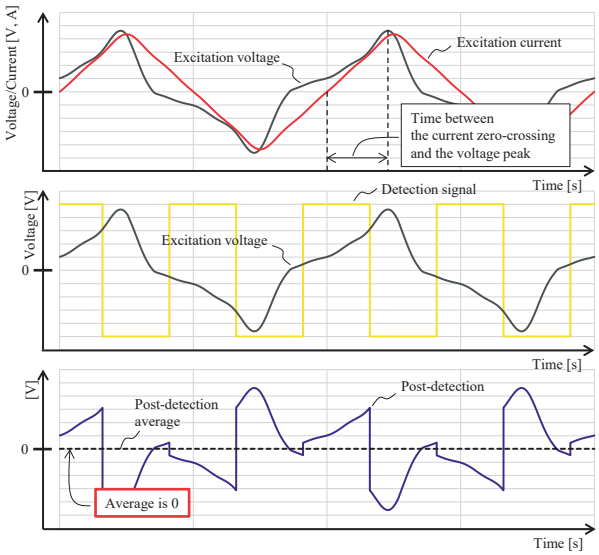

Figure 14 Excitation voltage waveform with no DC magnetic flux

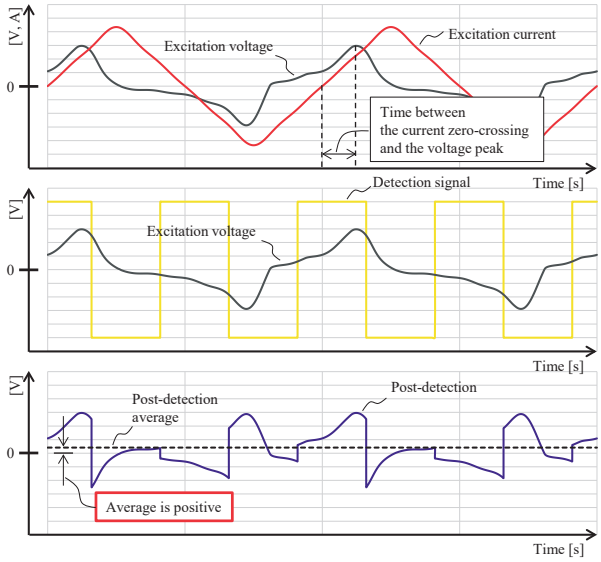

Figure 15 Excitation voltage waveform with DC magnetic flux applied

Problems and Countermeasures When Constructing an FG Sensor from an FPC

In general, FG sensors exhibit good DC characteristics, but when an FG sensor is made from an FPC, its temperature characteristics tend to deteriorate. Figure 16 shows an example of the excitation voltage waveform from an FG sensor with degraded temperature characteristics. Comparing the excitation voltage waveforms at ambient temperatures of −40°C and 85°C, it can be seen that the waveform changes significantly due to temperature variation. First, let us consider gain variation in this FG sensor. When the excitation voltage waveform changes, the amplitude of the second harmonic component generated when DC magnetic flux is applied to the FG sensor also changes; that is, the gain fluctuates. However, since the CT1000S operates by a zero-flux method, such gain fluctuations are compressed to a negligible level and do not pose a problem. Next, let us consider DC drift in this FG sensor. As described in the previous section, DC drift should not occur, based on the operating principle of the FG sensor. However, if there is a difference between the positive and negative slew rate characteristics of the amplifier that transmits the excitation voltage waveform, asymmetry arises in the waveform. This results in the generation of second harmonics. If the second harmonics remain constant across the entire temperature range, DC drift does not occur. However, as shown in Figure 16, if the excitation voltage waveform changes significantly due to temperature fluctuations, the amplitude of the second harmonics generated by the amplifier also varies, resulting in DC drift. Taking into account the slew rate characteristics of the amplifier transmitting the signal, it is preferable for the excitation voltage waveform of the FG sensor to exhibit minimal variation.

Such significant changes in the waveform are caused by the use of adhesive to fix the FPC and the magnetic material together during the FPC manufacturing process. When mechanical stress is applied to the magnetic material by adhesives and the like, the amount of stress varies with temperature, which in turn causes substantial changes in the magnetic permeability of the material and leads to variations in the excitation voltage waveform. To resolve this issue, the CT1000S adopts a structure that does not use adhesive between the FPC and the magnetic material. As a result, the benefits of using an FPC are retained while realizing an FG sensor with good temperature characteristics (Figure 17).

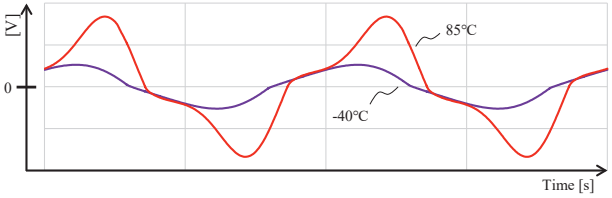

Figure 16 Example of excitation voltage waveform from FG sensor with degraded temperature characteristics

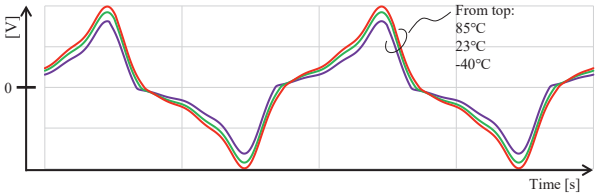

Figure 17 Example of excitation voltage waveform from FG sensor with good temperature characteristics

Reduction of FG Excitation Noise

As explained in the previous section, the FG sensor functions as a sensor through excitation. The magnetic flux generated by FG excitation links with the secondary winding, resulting in the appearance of signals unrelated to the primary current—namely, excitation noise—in the sensor output. For this reason, current sensors using FG sensors tend to have higher output noise and have been considered unsuitable for current waveform measurements. At present, current probes based on the Hall element detection method are widely used for current waveform measurement.

To enable use in current waveform measurement, the CT1000S reduces noise by adding a cancellation signal generated from the FG sensor's excitation signal to the sensor output (the noise cancellation signal generation circuit in Figure 11). This noise cancellation circuit reduces the amount of excitation noise to less than one-third. Figure 18 illustrates this effect. As a result, the CT1000S enables highly accurate current measurement not only with power meters but also with waveform measurement instruments such as oscilloscopes.

Figure 19 shows a comparison of output noise levels. While excitation noise is large in a conventional FG sensor and small in a Hall element sensor, the CT1000S achieves an output noise level comparable to that of a Hall element sensor despite incorporating an FG sensor.

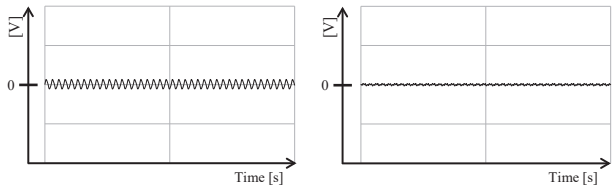

Figure 18 Before (left) and after (right) noise cancellation

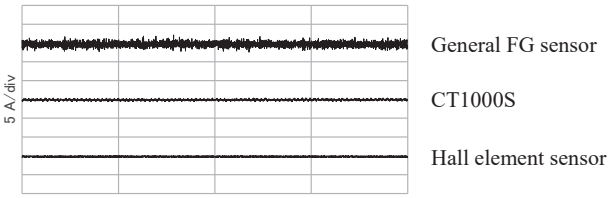

Figure 19 Comparison of output noise

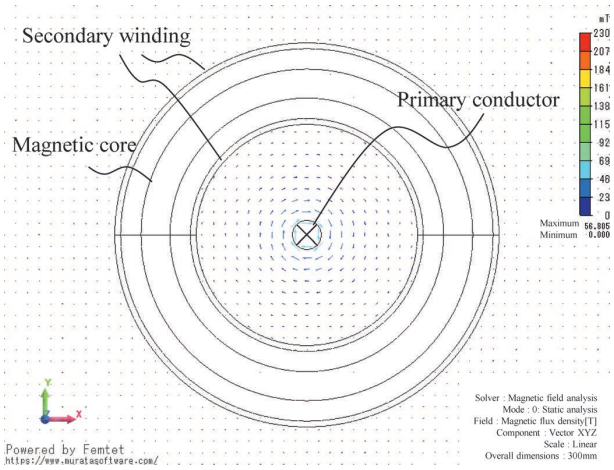

Figure 20 Magnetic flux density distribution when the primary conductor is centered on the through-hole

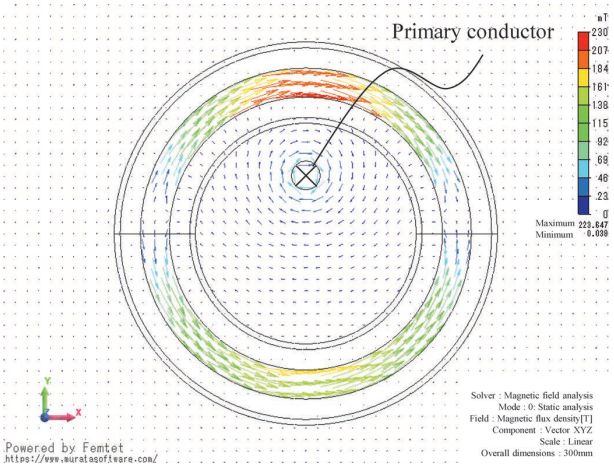

Figure 21 Magnetic flux density distribution when the primary conductor is offset from the through-hole

Effect of Primary Conductor Position

In general, the accuracy of clamp-type and through-type current sensors is specified for the case where the primary conductor is positioned at the center of the through-hole. This is because magnetic flux remains in the magnetic core even when operating by zero-flux if the primary conductor is not centered. Figure 20 shows simulation results when current is applied with the primary conductor centered in the through-hole and a current is applied to the secondary winding in the direction that cancels the flux. It can be seen that the magnetic flux in the core is effectively canceled and is almost zero. In contrast, Figure 21 shows simulation results when the current values in both the primary conductor and secondary winding are kept the same, but the primary conductor is offset from the center of the through-hole. Despite applying the same canceling current to the secondary winding, a significant amount of magnetic flux remains in the core. The secondary winding only cancels magnetic flux that circulates around the magnetic core. Therefore, it cannot cancel flux that diverges and converges without circulating the core, as occurs when the primary conductor is off-center. When this magnetic flux remains in the core and the flux density increases, the operating point of the magnetic circuit shifts, leading to degraded linearity, reduced gain, and increased measurement error.

Simulations were conducted to evaluate the extent to which such uncancelable magnetic flux would occur, and the necessary magnetic shielding structure and magnetic core cross-sectional area for the CT1000S were determined based on the results. As shown in Figure 22, the influence of the primary conductor position was small, but to reduce it further, a conductor position adjuster was employed (Figure 23). Figure 24 shows the variation in measurement values at a primary current frequency of 1 kHz, comparing cases with and without the conductor position adjuster. The results indicate that the influence of conductor position on measurement values is reduced to approximately one-third when the adjuster is used. This demonstrates that despite being a clamp-type sensor, the CT1000S is capable of achieving highly reproducible measurements.

Primary conductor position key
Variation evaluated relative to position (1)

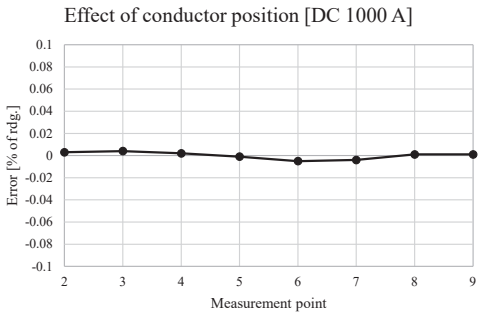

Figure 22 Effect of conductor position

Figure 23 Conductor position adjuster (left) and mounting illustration (right)

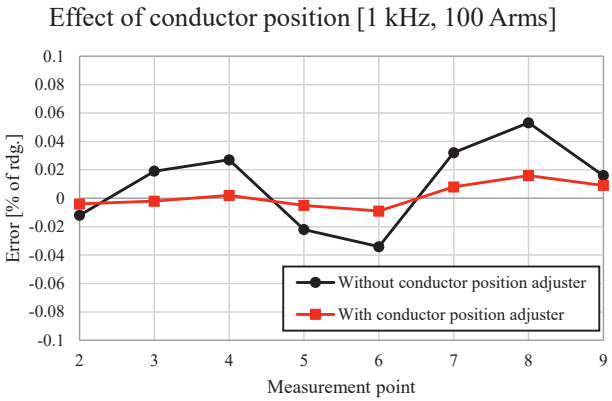

Figure 24 Effect of conductor position adjuster

Floating Structure with Cushioning Material

A protective structure is required to protect the internal sensor section from impacts in the event that the CT1000S main unit is accidentally dropped. In addition, to enhance measurement reproducibility, it is necessary to ensure sufficient engagement at the split section of the magnetic core in the closed position. To meet these needs, the CT1000S adopts a floating structure in which the internal components are supported by highly shock-absorbent cushioning material.

Figure 25 shows the details of the floating structure. The sensor section (light blue) is sandwiched between cushioning material (red) on all sides—top and bottom, inside and outside—and is securely held within the housing. This structure ensures that the sensor section is protected even when subjected to impact loads. Furthermore, by making the contact area of the outer cushioning material larger than that of the inner side, the sensor section is pushed inward, ensuring sufficient engagement at the split section.

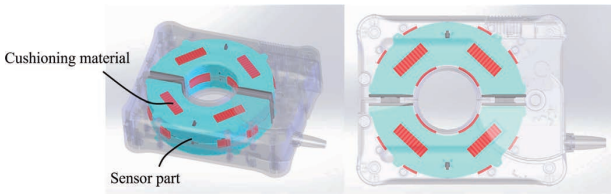

Figure 25 Floating structure

CONCLUSION

This paper described the features of the CT1000S AC/DC split-core current sensor, and the technologies realized in its development. The CT1000S can be used for both power measurement and waveform measurement, and it is our hope that it will contribute to the development of various devices aimed at realizing a decarbonized society.

REFERENCES

(1) Ministry of Economy, Trade and Industry, FY2022 Annual Report on Energy (Energy White Paper 2023), 2024 (in Japanese)
(2) Katsuaki Suganuma, Hiroshi Yamaguchi, et al., System Integration of Wide Band Gap Semiconductors, CMC Publishing, 2016 (in Japanese)
(3) Toshihiko Iwata, "Cooperative Energy Management System Utilizing EV and PV," Mitsubishi Denki giho, Vol. 93, No. 7, 2019, pp. 35-38 (in Japanese)